minerals

MDPI

Article

Textures and Chemical Compositions of Nb-Bearing Minerals and Nb Mineralization in the Shuangshan Nepheline Syenite Pluton, East Qinling, China

Hong Wang [1,2], Yong Tang [1,*], Yu-Sheng Xu [1,2], Hui Zhang [1], Zheng-Hang Lv [1], Shan-Xian Qin [1,2] and Ying-Wei Song [3]

[1] Key Laboratory of High-Temperature and High-Pressure Study of the Earth's Interior, Institute of Geochemistry, Chinese Academy of Sciences, Guiyang 550081, China; wang-hong@mail.gyig.ac.cn (H.W.); xuyusheng20@mails.ucas.ac.cn (Y.-S.X.); zhanghui@mail.gyig.ac.cn (H.Z.); Lvzhenghang@mail.gyig.ac.cn (Z.-H.L.); tanshanxian@mail.gyig.ac.cn (S.-X.Q.)
[2] University of Chinese Academy of Sciences, Beijing 100049, China
[3] Henan Institute of Geological Sciences, Zhengzhou 450001, China; songyingwei1974@163.com
* Correspondence: tangyong@vip.gyig.ac.cn; Tel.: +86-851-84394846

Abstract: The Shuangshan alkaline complex located in the Henan province of China is a newly discovered, potentially giant niobium (Nb) deposit. A variety of Nb-bearing minerals including pyrochlore, zircon, and titanite have been identified in this deposit. Distinct textural and chemical differences of pyrochlore and zircon indicate that both have different origins. The magmatic pyrochlore and zircon both have euhedral grains with small sizes. On the other hand, hydrothermal pyrochlore is mainly intergrown on the edge or inside of hydrothermal zircon in the form of an aggregate. Compared with magmatic pyrochlore, the contents of F, Ca, and Na in hydrothermal pyrochlore are obviously high. The texture and composition of hydrothermal pyrochlore and zircon indicate that Ca-bearing hydrothermal alteration resulted in the migration of Nb from Nb-bearing zircon and the reprecipitation of Nb to form aggregate pyrochlore. However, the quantitative calculation shows that the amount of Nb migrated from zircon is very small. Therefore, this study suggests that hydrothermal alteration plays a certain role in the redistribution of Nb, but the enrichment of Nb is limited.

Keywords: alkaline complex; Nb deposit; pyrochlore; zircon; alteration

Citation: Wang, H.; Tang, Y.; Xu, Y.-S.; Zhang, H.; Lv, Z.-H.; Qin, S.-X.; Song, Y.-W. Textures and Chemical Compositions of Nb-Bearing Minerals and Nb Mineralization in the Shuangshan Nepheline Syenite Pluton, East Qinling, China. *Minerals* **2021**, *11*, 1163. https://doi.org/10.3390/min11111163

Academic Editor: Massimo D'Antonio

Received: 24 September 2021
Accepted: 15 October 2021
Published: 21 October 2021

1. Introduction

Although alkaline igneous rocks constitute only a small part of the Earth's crust in volume, they have gained considerable attention recently. One important reason for this is that they are extremely rich in high-field strength elements (HFSE), Zr, Nb, Y, and Rare Earth Elements (REEs) [1]. These elements, also known as critical metals, are widely used in "high-tech" applications, such as defense systems, high-strength and corrosion-resistant alloys, and energy generation and storage [2]. In most cases, the enrichment of HFSE is associated with a multi-stage process. These elements behave incompatibly during most magmatic processes, and thus, the first step toward ore formation usually involves magma formed as the product of extensive fractional crystallization [3]. The subsequent upgrading of metal concentrations has been attributed to a series of processes, including liquid immiscibility [4,5], magmatic crystal accumulation [6,7], and in particular, hydrothermal alteration [8–12].

Many peralkaline igneous complexes display evidence of hydrothermal alteration, particularly in the parts most enriched in HFSE. At present, in alkaline granite-syenite deposits, the hydrothermal process may have two main functions. First, the hydrothermal process may be the dominant mechanism leading to the mineralization of HFSE. For example, the mineralization of HFSE in Strange Lake, Canada was explained by the orthomagmatic fluid transport of these elements as fluoride complexes and their subsequent deposition resulting from mixing with an externally derived Ca-rich meteoric fluid [11]. Second, the hydrothermal process just redistributes HFSE into secondary minerals that are more amenable to beneficiation than their magmatic precursors. For instance, a part of Nb-bearing minerals, including columbite and fergusonite-(Y) in the Nechalacho deposit in Canada was produced by the alteration of the cores of Nb-enriched zircon and eudialyte [7,13,14].

The Shuangshan alkaline complex located in the Henan province of China is a newly discovered, potentially giant niobium deposit which is hosted by an alkaline igneous suit. The Nb_2O_5 concentration in this suit is in the range of 0.05–0.10 wt.% [15]. In recent years, some studies have examined the petrology, geochemistry, and geochronology of the host rocks of the Shuangshan Nb deposit [16,17]. However, the metallogenic mechanism of Nb has not yet been investigated. The purpose of this study is to use the textural relationships and compositions of the Nb-bearing minerals of the Shuangshan deposit to investigate the role of primary magmatic and hydrothermal metasomatic processes in their crystallization and determine the extent of remobilization of Nb. In doing so, this paper proposes a model explaining the genesis of the Shuangshan deposit, which can be applied to study similar deposits elsewhere.

2. Geological Setting

2.1. Regional Geology

The Shuangshan Nb deposit in Henan province in central China is situated in the Qinling Orogenic Belt (QOB). The QOB is a major composite collisional zone located between North China (NC) and South China (SC) (Figure 1a). From north to south, the QOB can be divided into four tectonic belts by sutures and faults: the Southern North China Block (S-NCB), North Qinling Belt (NQB), South Qinling Belt (SQB), and Northern South China Block (N-SCB) (Figure 1b). The QOB has been formed by multiple tectonic movements from the Grevillian-aged to the Late Mesozoic-Cenozoic intracontinental orogeny. The detailed orogenetic history of the QOB can be found in the work of Dong and Santosh [18].

The Shuangshan alkaline complex, which comprises a series of alkaline silica- undersaturated syenite and silica-oversaturated granite, hosts the Shuangshan Nb deposit. This complex, located in the eastern margin of the S-NCB and NQB, intrudes into the Neoproterozoic Luanchuan Group sericite-quartz schist. This complex was emplaced between 867 and 833 Ma based on the U-Pb ages of zircon and titanite [16]. Neoproterozoic plutons are widespread across the NQB and were formed in two stages with diverse geochemistry, geochronology, and structures [19]. The first-stage granite formed in ca. 979–911 Ma, has an S-type geochemical feature, and displays strong deformation, whereas the second stage granite (ca. 889–844) shows A-type geochemical affinity and weak formation. The formation of two-stage plutons was related to the Grevillian-aged orogeny situated between the North Qinling terrane and the North China Block, indicating a transition of the tectonic setting from subduction, collision, and post-collisional collapse and extension [16]. The Shuangshan alkaline complex was formed in a post-collisional extensional setting [16,17].

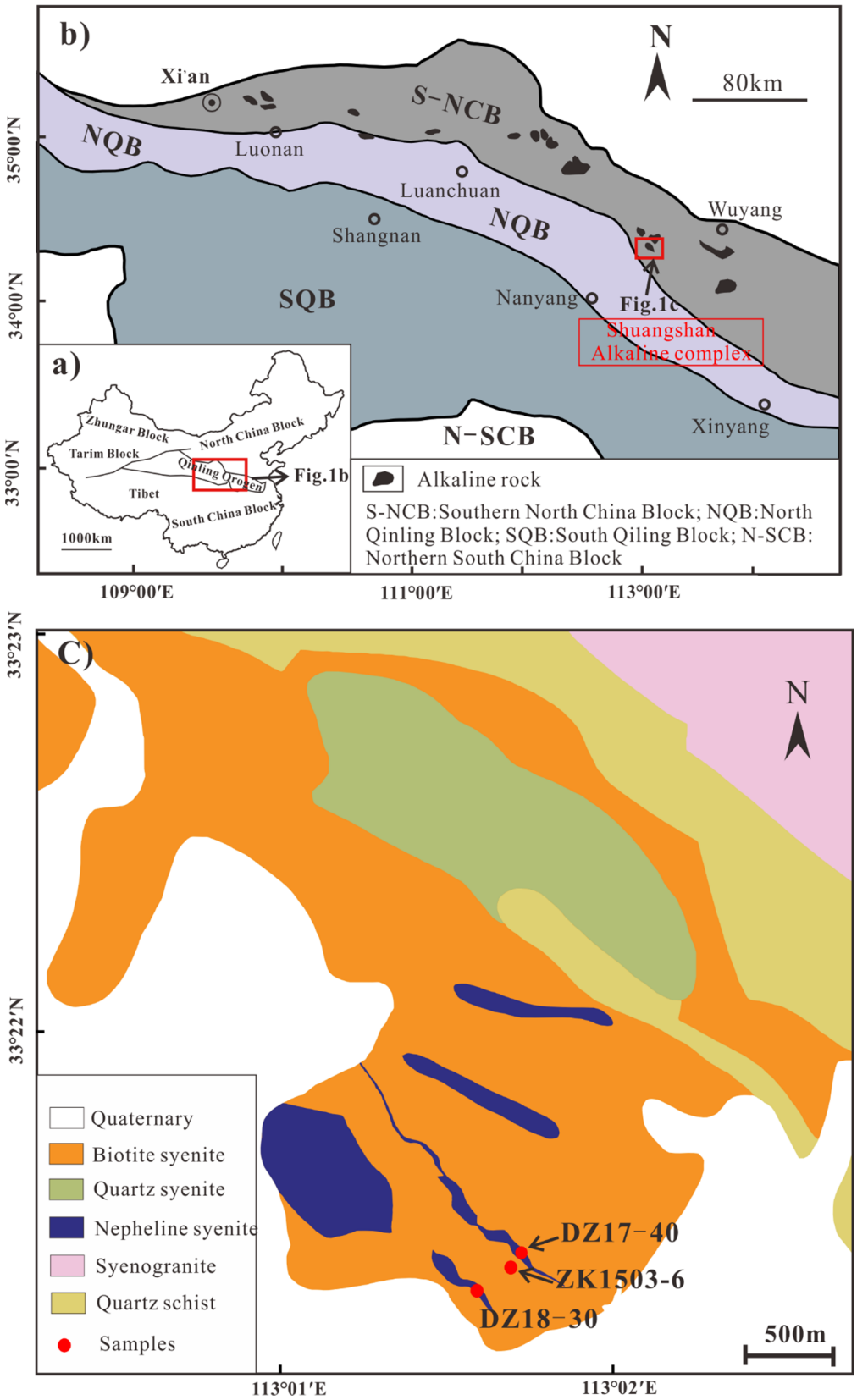

Figure 1. (**a**) Location of the Qinling Orogenic Belt. (**b**) A geological sketch map of the Qinling Orogenic Belt and distribution of alkaline rocks in the NCB (modified after Zhang et al., 2002) [20]; (**c**) A geological map of the Shuangshan alkaline complex, showing the distribution of the principal rock types and the location of the samples.

2.2. Shuangshan Alkaline Complex

The Shuangshan alkaline complex constitutes a part of the East Qinling Alkaline Rock Belt, which starts from Pingwu in the east, passes through Fangcheng and Luanchuan, and ends in Luonan, Shaanxi with a length of more than 400 km [21]. The complex mainly consists of biotite syenite, nepheline syenite, quartz syenite, and syenogranite. The exposed area of this complex is approximately 20 km^2, which is irregular in quaternary sediments (Figure 1c).

Biotite syenite with a fine-grained gneissic structure is the main component of the complex. The rock-forming minerals of biotite syenite are alkali feldspar (60–75 vol.%), biotite (10–15 vol.%), and albite (5–10 vol.%). The accessory minerals included euhedral (envelope-shaped) titanite, calcite, and apatite (Figure 2a,b). Alkali feldspar and albite are euhedral-subhedral. Biotite is flaky and mostly oriented. Dissolution holes were found in titanite grains filled with zircon and unrecognized Nb-bearing minerals.

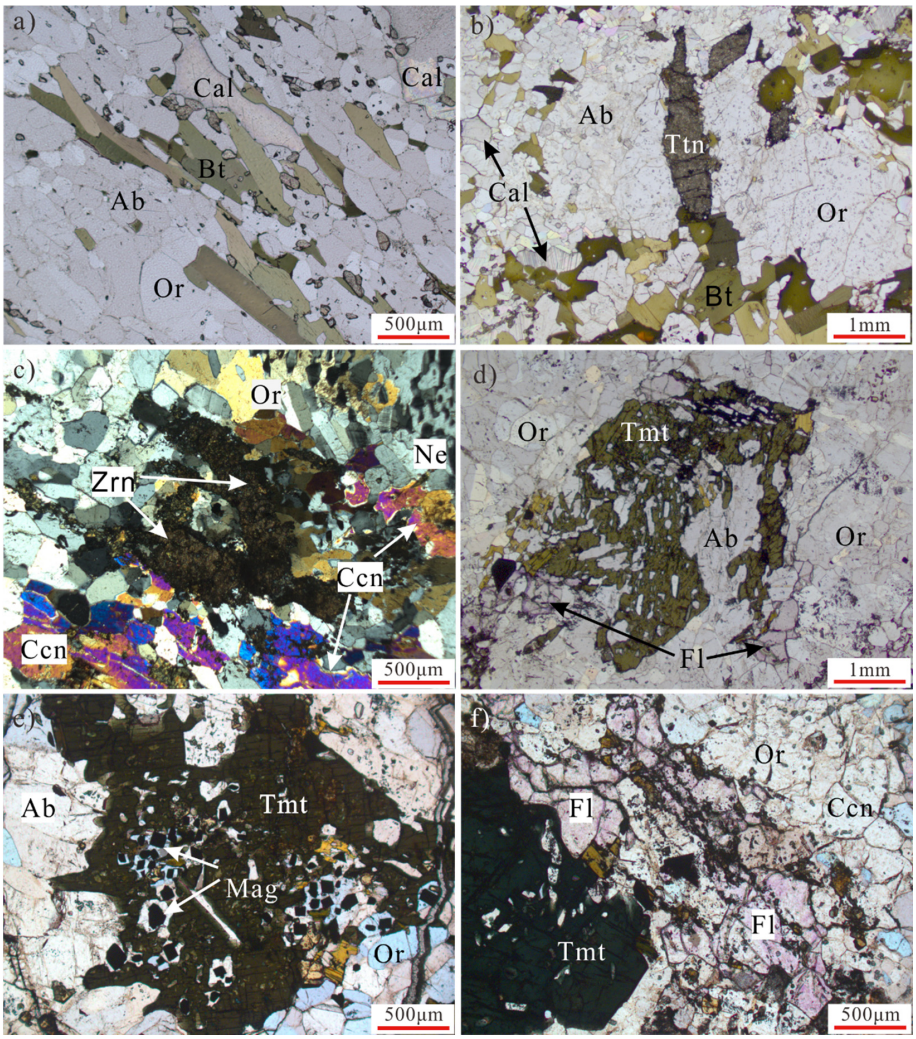

Figure 2. Petrography of the Shuangshan alkaline complex. (**a**) Sheet biotite. (Bt), orthoclase (Or), albite (Ab), and a small amount of calcite (Cal) in the fine-grained gneissic structure biotite syenite. (**b**) Envelope-shaped titanite (Ttn) in biotite syenite. (**c**) Nepheline (Ne), cancrinite (Ccn), orthoclase, and zircon (Zrn) aggregate in nepheline syenite (cross-polarized light). (**d**) Orthoclase, albite, subhedral fluorite (Fl), and taramite (Tmt) with a diablastic texture in nepheline syenite. (**e**) Subhedral taramite with magnetite (Mag) in it. The taramite is associated with orthoclase and albite in nepheline syenite. (**f**) Disseminated fluorite, cancrinite, orthoclase, and subhedral taramite in nepheline syenite.

Nepheline syenite outcrops mostly in the central zone of biotite syenite, displaying a gradual transition relationship with it. Nepheline syenite shows medium-to-fine-grained and rock-forming minerals, including alkali feldspar (50–60 vol.%), albite (10–25 vol.%), nepheline (15–20 vol.%), taramite (5–10 vol.%), and fluorite (1–3 vol.%). The accessory minerals in nepheline syenite include pyrochlore, zircon, titanite, garnet, allanite, calcite, gittinsite, and magnetite. Alkali feldspar is mainly composed of euhedral orthoclase and minor microcline. Nepheline crystals are generally euhedral-subhedral and mainly associated with cancrinite, which is faint yellow to bright purple in color (Figure 2c). All taramite in nepheline syenite is subhedral-anhedral with a diameter of approximately 1–2 mm, generally showing a diablastic texture (Figure 2d). In addition, in sample DZ18-21, euhedral magnetite crystals are observed in the taramite grains (Figure 2e). The subhedral-anhedral fluorites in the sample are light purple, and most of them are subhedral-anhedral and distribute between the grains of feldspar and nepheline (Figure 2f).

Quartz syenite and syenogranite are less abundant and cross-cut the external parts of the complex (Figure 1c). A single aegirine-augite syenite is locally enclosed in the complex [17].

The Shuangshan alkaline complex originated from the melting of a small proportion of enriched mantle and has been contaminated to varying degrees by crust materials during emplacement, according to the isotopic data of Bao et al. (2008) and Zhu et al. (2020). After the emplacement of alkaline basaltic magma, silica-undersaturated rocks (nepheline and biotite syenite) were directly differentiated during the continuous evolution of magma. However, silica-oversaturated rocks (quartz syenite and syenite granite) situated north of the complex were formed by the magma with high differentiation, contaminated by the crust materials according to the εNd(t) values (from -0.7 to -1.5 and from -4.5 to -4.9) of nepheline and biotite syenite as well as syenite granite and quartz syenite, respectively [16].

3. Samples and Analytical Methods

The highest concentrations of Nb were found in nepheline syenite; thus, it was the mineral mainly sampled in this study. A total of 10 samples, including drill holes and two different outcrop samples (Figure 1c), were collected for mineralogical and mineral chemistry analyses.

Backscattered electron image (BSE) observations and electron probe microanalysis (EPMA) were carried out at the State Key Laboratory of Ore Deposit Geochemistry of the Chinese Academy of Sciences. The compositions of nepheline, taramite, zircon, titanite, and pyrochlore were analyzed using a jxa8530F-plus electron microprobe with an acceleration voltage of 25 kV and a 10-nA beam current. For rock-forming minerals such as taramite and nepheline, the diameter of the beam was 10 μm, and the diameter of the pyrochlore and zircon beam was 2–3 μm. Data reduction was performed using the ZAF correction method. The standard minerals and measurement conditions for each mineral are provided in Appendix A (Table A1).

4. Results

4.1. Pyrochlore

Pyrochlore is mainly found in nepheline syenite and is also the main ore mineral found in the study area. Based on its morphology and paragenetic assemblages, it can be divided into two types as follows. Type-1 pyrochlore is generally found in orthoclase and albite grains, with its crystals being shaped like hexagonal or regular polygons (Figure 3a,b). The diameter of type-1 pyrochlore is small (mostly between 10 and 50 μm). In addition, most euhedral pyrochlore grains have overgrown pyrochlore on their surfaces (Figure 3b). Contrarily, type-2 pyrochlore is the main form of pyrochlore and is mostly associated with aggregate zircon ± allanite ± magnetite, where the diameters of large mineral aggregates can reach 2 mm (Figure 3c,d). Nearly all aggregate mineral assemblages of pyrochlore ± zircon ± allanite ± magnetite are found in the mineral grains of cancrinite or adjacent to cancrinite.

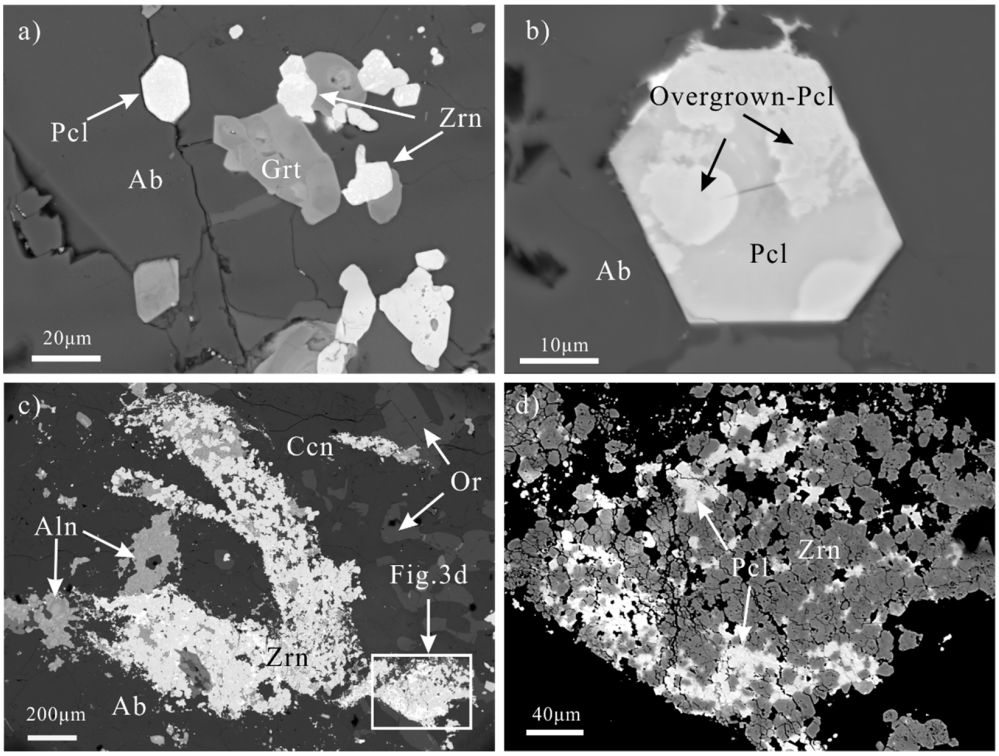

Figure 3. Backscattered electron (BSE) image of Nb-bearing mineral assemblage in a nepheline syenite. (**a**) Type-1 pyrochlore (Pcl) and zircon (Zrn) association with garnet (Grt). (**b**) Type-1 pyrochlore crystal overgrown by a Ca-Na-rich pyrochlore. (**c**) Aggregate allanite (Aln) and type-2 zircons distributed in cancrinite and alkaline feldspar. (**d**) Type-2 pyrochlores rich in aggregate zircon.

The elemental composition based on the EPMA analysis (Table 1) showed that the total contents of type-1 and type-2 pyrochlores were in the range of 90.12–94.74 wt.% (average: 92.80 wt.%) and 94.36–98.62 wt.% (average: 96.63 wt.%), respectively. Based on chemical composition, the calculated chemical formulas of type-1 and type-2 pyrochlores are $(U_{0.02–0.03}, Y_{0–0.01}, Pb_{0–0.01}, Fe_{0.01–0.03}, Mn_{0–0.03}, Sr_{0.01–0.04}, Ca_{0.74–0.85}, K_{0.02–0.04}, Na_{0.02–0.16},)(Nb_{1.11–1.34}, Ta_{0.03–0.04}, Ti_{0.27–0.32}, Si_{0.24–0.44}, Al_{0.06–0.15})(OH_{0.76–0.82}, F_{0.18–0.24})$ and $(U_{0.02–0.03}, Y_{0–0.01}, Pb_{0–0.01}, Fe_{0–0.01}, Sr_{0–0.01}, Ca_{1.11–1.21}, Na_{0.53–0.61},)(Nb_{1.57–1.61}, Ta_{0.03–0.04}, Ti_{0.35–0.38}, Si_{0–0.01}, Al_{0–0.01})(OH_{0.35–0.55}, F_{0.45–0.65})$, respectively. The average concentrations of Na_2O, CaO, and F of type-1 pyrochlore were 1.51, 15.13, and 1.49 wt.%, respectively, and the SiO_2 concentration was found to be 2.83–8.83 wt.%, with the average concentration being 5.11 wt.%. The Na_2O, CaO, and F average concentrations in the type-2 pyrochlore were higher than those of the type-1 pyrochlore, with the average values being 4.44 wt.%, 17.45 wt.%, and 2.54 wt.%, respectively. Furthermore, the SiO_2 concentration was found to be lower, being less than 1 wt.%. In addition, the overgrown pyrochlore showed a composition between the type-1 pyrochlore and type-2 pyrochlore (Figure 4).

Table 1. Major elements of representative pyrochlores of the Shuangshan nepheline syenite (wt.%).

Pyrochlore Type	**Type-1 Pyrochlore**				**Type-2 Pyrochlore**				**Overgrown Pyrochlore**		
Sample No.	1	2	3	4	5	6	7	8	9	10	11
Nb_2O_5	56.17	54.39	49.70	50.53	60.63	59.06	59.44	59.78	55.74	56.82	59.34
Ta_2O_5	2.56	2.83	2.31	2.17	1.86	2.39	2.49	2.05	2.62	2.57	2.08
TiO_2	8.06	7.88	7.28	7.30	8.54	8.61	7.71	8.61	8.09	8.45	8.39
SiO_2	4.62	5.88	8.83	7.52	-	0.13	-	0.12	2.61	1.16	-
Al_2O_3	0.94	1.31	2.60	1.89	-	0.06	0.05	0.12	0.75	0.17	0.05
FeO	0.74	0.77	0.12	0.46	-	-	0.25	-	-	-	0.10

Table 1. *Cont.*

Pyrochlore Type	Type-1 Pyrochlore				Type-2 Pyrochlore				Overgrown Pyrochlore		
Sample No.	1	2	3	4	5	6	7	8	9	10	11
MnO	0.59	0.53	0.04	0.76	0.03	-	-	0.03	0.15	0.06	-
Na_2O	0.64	0.16	1.42	1.58	5.12	4.70	5.29	4.67	3.92	4.50	5.75
Y_2O_3	0.20	0.13	0.30	0.40	0.37	0.39	0.25	0.39	0.51	0.46	0.33
SrO	1.14	1.19	0.40	0.40	0.06	0.09	0.28	0.04	0.07	0.18	0.04
K_2O	0.60	0.42	0.58	0.32	-	-	-	0.02	0.12	0.02	-
CaO	14.97	14.00	13.89	15.07	17.88	17.79	18.79	17.69	16.27	15.95	17.70
UO_2	1.59	1.99	2.38	1.68	1.84	1.79	1.65	1.93	2.42	2.35	1.85
PbO	0.41	0.32	0.37	0.58	0.44	0.39	0.38	0.45	0.49	0.37	0.44
F	1.27	1.08	1.53	1.42	2.75	2.61	3.43	2.43	1.83	2.03	3.39
H_2O*	2.24	2.39	2.31	2.22	1.27	1.31	0.87	1.42	1.79	1.59	0.93
F=O	0.53	0.45	0.64	0.60	1.15	1.10	1.44	1.02	0.77	0.85	1.42
Total	96.19	94.80	93.45	92.08	99.66	98.25	99.45	98.72	96.63	95.84	98.96
Structural Formulae											
Nb	1.34	1.27	1.11	1.18	1.60	1.57	1.61	1.58	1.42	1.51	1.59
Ta	0.04	0.04	0.03	0.03	0.03	0.04	0.04	0.03	0.04	0.04	0.03
Ti	0.32	0.31	0.27	0.28	0.37	0.38	0.35	0.38	0.34	0.37	0.37
Si	0.24	0.30	0.44	0.39	-	0.01	-	0.01	0.15	0.07	-
Al	0.06	0.08	0.15	0.12	-	-	-	0.01	0.05	0.01	-
Fe	0.03	0.03	0.01	0.02	-	-	0.01	-	-	-	0.01
Mn	0.03	0.02	-	0.03	-	-	-	-	0.01	-	-
Na	0.07	0.02	0.14	0.16	0.58	0.54	0.61	0.53	0.43	0.51	0.66
Y	0.01	-	0.01	0.01	0.01	0.01	0.01	0.01	0.02	0.01	0.01
Sr	0.04	0.04	0.01	0.01	-	-	0.01	-	-	0.01	-
K	0.04	0.03	0.04	0.02	-	-	-	-	0.01	-	-
Ca	0.85	0.78	0.74	0.84	1.12	1.12	1.21	1.11	0.98	1.00	1.12
U	0.02	0.02	0.03	0.02	0.02	0.02	0.02	0.03	0.03	0.03	0.02
Pb	0.01	-	0.01	0.01	0.01	0.01	0.01	0.01	0.01	0.01	0.01
F	0.21	0.18	0.24	0.23	0.51	0.49	0.65	0.45	0.33	0.38	0.63
OH	0.79	0.82	0.76	0.77	0.49	0.52	0.35	0.55	0.67	0.62	0.37

Note. Calculated on the basis of 2 B site cations. (-) is below detection limit. H_2O* is calculated based on the content of OH.

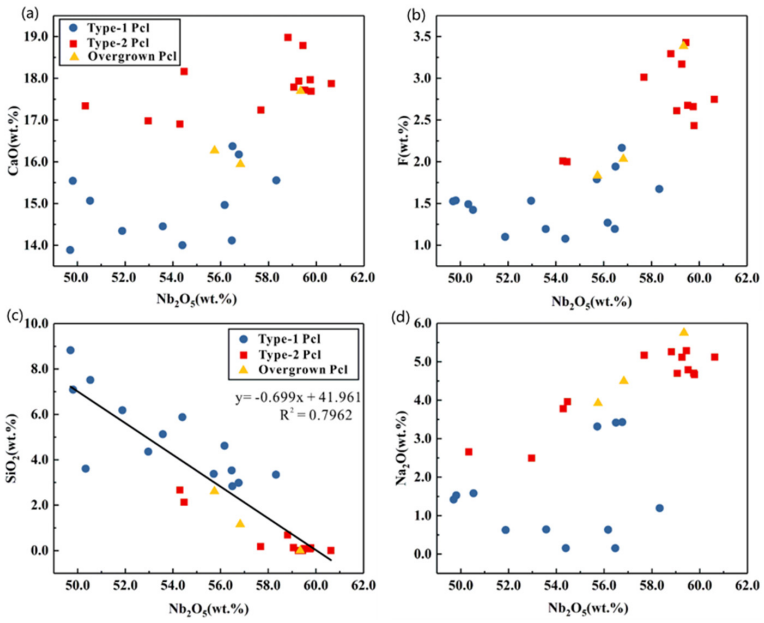

Figure 4. Major element compositions of pyrochlore in the Shuangshan nepheline syenite as a function of the Nb_2O_5 (wt.%) concentration: (**a**) CaO, (**b**) F, (**c**) SiO_2, and (**d**) Na_2O.

4.2. Zircon

Based on its morphology and paragenetic assemblage, zircon in the Shuangshan nepheline syenite can also be divided into two types. Type-1 zircon is a euhedral zircon, which is less abundant and mainly found in alkaline feldspar mineral grains. The diameter of this type of zircon crystal is approximately 20–50 μm, and it has a short columnar crystal with a clean surface but generally has dissolution cavities in the core (Figure 5a). Type-2 zircon was found as an irregular aggregate. The surface of the subhedral-anhedral zircon generally showed dissolution cavities (Figure 5b). Type-2 zircon is yellowish brown to brown, with the diameter of the aggregate reaching the millimeter scale. This type of zircon is associated with allanite ± pyrochlore ± magnetite ± gittinsite, and some zircons are scattered in the interior and periphery of the allanite mineral aggregate (Figure 5c,d). In addition, type-2 zircon contains the pyrochlore aggregate and a small amount of gittinsite on its margin, and this type of zircon was mainly found in the mineral grains of cancrinite (Figures 2c and 3c,d).

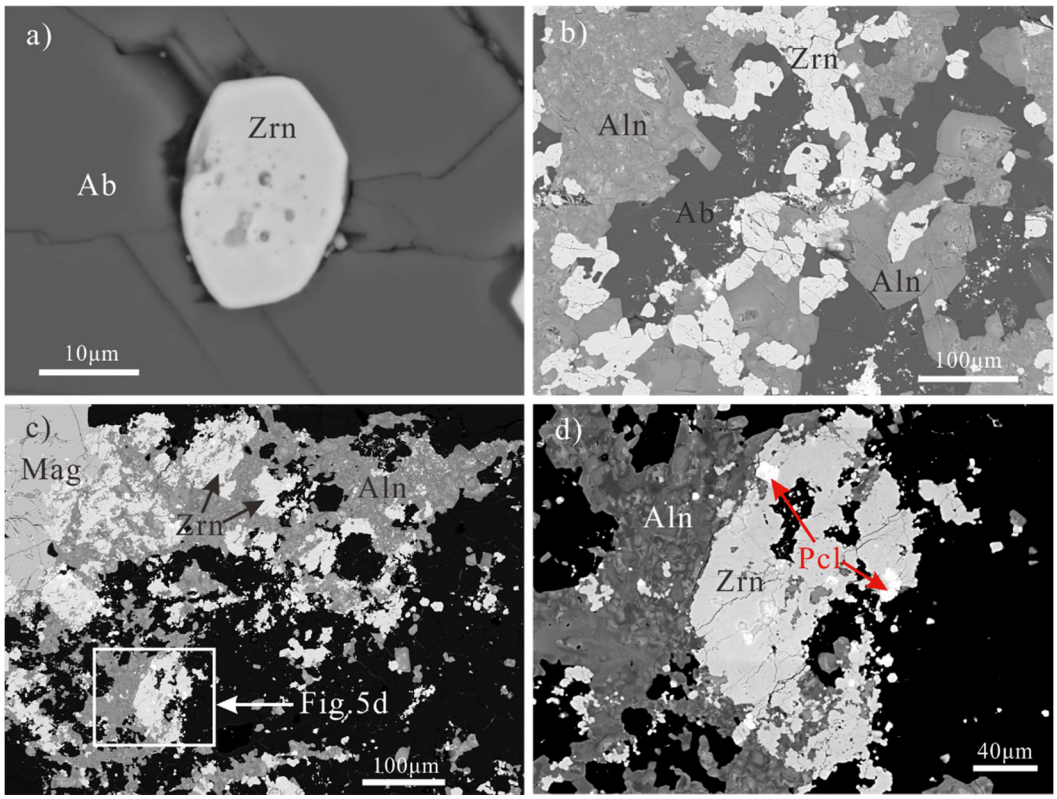

Figure 5. BSE image of zircon with different paragenetic assemblages from nepheline syenite. (**a**) Type-1 zircon grain with slight dissolution pores in the core. (**b**) Type-2 zircons accompanied by subhedral allanite (Aln). (**c**) Type-2 zircon associated with allanite and magnetite (Mag). (**d**) Type-2 pyrochlore (bright white mineral) in type-1 zircon, and this type of zircon is accompanied by subhedral allanite in rock-forming minerals.

The chemical compositions of the two types of zircons are shown in Table 2. The results showed that the total content of zircons was in the range of 98–100 wt.%. The concentration of Nb_2O_5 in type-1 zircon ranged from 200 to 2100 ppm. For the type-2 zircon, the Nb_2O_5 concentration ranged from 510 to 3900 ppm. The concentration of Nb_2O_5 in different types of zircons in nepheline syenite did not regularly change, and it varied over a large range (Figure 6).

Table 2. Major elements of representative zircon of the Shuangshan nepheline syenite (wt.%).

No.	1	2	3	4	5	6	7	8	9	10	11	12	13	14	15	16	17	18	19	20
ZrO_2	63.46	64.63	63.65	64.78	64.05	63.69	64.99	63.63	63.05	64.63	63.44	62.43	62.83	63.32	64.36	64.36	63.77	64.21	64.57	64.13
Nb_2O_5	0.09	0.10	0.39	0.12	0.05	0.07	0.16	0.11	0.09	0.09	0.21	0.14	0.13	0.15	0.16	0.08	0.07	0.06	0.02	0.06
CaO	0.02	0.05	0.08	0.03	0.02	0.04	0.08	0.02	0.04	0.03	0.02	0.02	0.08	0.01	0.02	0.01	0.04	0.04	0.03	0.01
Y_2O_3	-	-	0.19	-	0.08	0.17	-	0.01	-	-	0.21	0.23	0.15	0.06	0.15	-	-	0.10	-	-
SiO_2	33.55	33.66	33.43	33.82	33.63	33.88	33.58	33.41	33.46	33.40	33.94	34.02	34.12	34.07	33.96	33.63	33.65	33.26	33.92	33.80
La_2O_3	-	-	-	-	-	-	0.06	-	0.04	-	-	-	-	0.05	-	-	-	0.06	-	-
Ce_2O_3	-	-	-	-	-	0.03	-	-	0.03	-	-	-	-	0.05	0.03	-	-	0.03	-	-
HfO_2	1.39	1.34	1.31	1.43	1.35	1.36	1.41	1.37	1.39	1.46	1.12	1.08	1.28	1.34	1.27	1.40	1.25	1.25	1.43	1.23
Total	98.51	99.78	99.05	100.18	99.18	99.24	100.28	98.55	98.1	99.61	98.94	97.92	98.59	99.05	99.95	99.48	98.78	99.01	99.97	99.23
Structural Formulae																				
Zr	0.953	0.960	0.952	0.959	0.956	0.949	0.963	0.956	0.951	0.964	0.946	0.937	0.938	0.943	0.953	0.959	0.954	0.963	0.956	0.955
Nb	0.001	0.001	0.005	0.002	0.001	0.001	0.002	0.002	0.001	0.001	0.003	0.002	0.002	0.002	0.002	0.001	0.001	0.001	-	0.001
Ca	0.001	0.002	0.003	0.001	0.001	0.001	0.003	0.001	0.001	0.001	0.001	0.001	0.003	-	0.001	-	0.001	0.001	0.001	-
Y	-	-	0.003	-	0.001	0.003	-	-	-	-	0.003	0.004	0.002	0.001	0.002	-	-	0.002	-	-
Si	1.033	1.026	1.026	1.026	1.030	1.035	1.020	1.029	1.035	1.021	1.038	1.048	1.045	1.041	1.031	1.027	1.033	1.023	1.030	1.033
La	-	-	-	-	-	-	0.001	-	-	-	-	-	-	0.001	-	-	-	0.001	-	-
Ce	-	-	-	-	-	-	-	-	-	-	-	-	-	0.001	-	-	-	-	-	-
Hf	0.012	0.012	0.011	0.012	0.012	0.012	0.012	0.012	0.012	0.013	0.010	0.009	0.011	0.012	0.011	0.012	0.011	0.011	0.012	0.011

Note. Atoms per formula units (apfu) are based on 4 oxygens. (-) is below the detection limit. 1–10: type-2 zircon; 11–20: type-1 zircon.

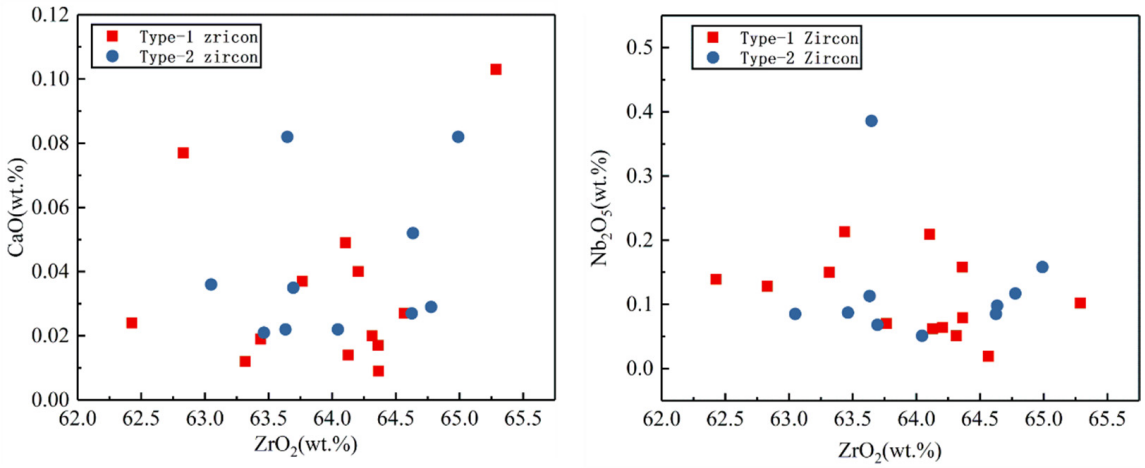

Figure 6. Major element compositions of zircon in the Shuangshan nepheline syenite as a function of the ZrO_2 (wt.%) concentration: (**right**) Nb_2O_5 and (**left**) CaO.

4.3. Titanite

Titanite is another important Nb-bearing mineral found in the nepheline syenite, with its main distribution found in cancrinite and orthoclase. It often coexists with allanite. Titanite is irregular, with the size of the mineral reaching the millimeter grade. It has a harbor-like corrosion structure. Additionally, small pyrochlore crystals (~10 μm) exist in the titanite grains. Other minerals associated with titanite include zircon, magnetite, and allanite mineral aggregates.

The composition of titanite is listed in Table 3. The concentration of Nb_2O_5 in titanite was in the range of 1.03–1.63 wt.%, and the calculated chemical formula was $Ca_{0.96–0.97}$, $Y_{0–0.01}$, $Mn_{0–0.01}$, $Ti_{0.67–0.76}$, $Al_{0.19–0.28}$, $Fe_{0.06–0.08}$, $Nb_{0.01–0.02}$, $Si_{0.98–0.99}$, $O_4[O_{0.72-0.82}$, $F_{0.18–0.24}$, $(OH)_{0.01–0.06}]$.

Table 3. Major elements of representative titanite of the Shuangshan nepheline syenite (wt.%).

No.	1	2	3	4	5	6	7	8	9	10
Nb_2O_5	1.12	1.57	1.63	1.51	1.52	1.22	1.39	1.10	1.03	1.53
TiO_2	27.71	27.68	28.43	28.35	29.03	28.31	31.21	28.26	29.91	29.30
Al_2O_3	7.41	7.35	6.94	6.75	6.40	7.15	4.87	7.15	6.05	6.33
Y_2O_3	0.40	0.35	0.35	0.34	0.38	0.34	0.56	0.32	0.25	0.39
SiO_2	30.85	30.85	30.71	30.76	30.74	30.83	30.38	30.71	30.81	30.59
Fe_2O_3	1.12	1.10	1.08	1.09	1.06	1.12	1.39	1.12	1.10	1.05
CaO	28.20	28.13	27.91	28.21	28.21	28.33	27.69	28.32	28.26	27.96
MnO	0.23	0.23	0.22	0.21	0.20	0.25	0.16	0.22	0.23	0.17
F	2.36	2.09	2.33	2.05	1.90	2.00	1.69	2.28	1.73	1.77
F=O	0.99	0.88	0.98	0.86	0.80	0.84	0.71	0.96	0.73	0.74
Total	98.41	98.47	98.61	98.41	98.65	98.70	98.62	98.51	98.65	98.33
				Structural Formulae						
Nb	0.02	0.02	0.02	0.02	0.02	0.02	0.02	0.02	0.01	0.02
Ti	0.67	0.67	0.69	0.69	0.70	0.68	0.76	0.68	0.72	0.71
Al	0.28	0.28	0.26	0.26	0.24	0.27	0.19	0.27	0.23	0.24
Y	0.01	0.01	0.01	0.01	0.01	0.01	0.01	0.01	-	0.01
Si	0.99	0.99	0.99	0.99	0.99	0.99	0.98	0.99	0.99	0.99
Fe	0.06	0.06	0.06	0.06	0.06	0.06	0.08	0.06	0.06	0.06
Ca	0.97	0.97	0.96	0.97	0.97	0.97	0.96	0.97	0.97	0.97
Mn	0.01	0.01	0.01	0.01	0.01	0.01	-	0.01	0.01	-
F	0.24	0.21	0.24	0.21	0.19	0.20	0.17	0.23	0.18	0.18
(O,OH)	0.76	0.79	0.76	0.79	0.81	0.80	0.83	0.77	0.82	0.82

Note: calculated on the basis of 3 cations.

4.4. Allanite

Accessory minerals in nepheline syenite also include allanite, which was mainly found as subhedral aggregates, as shown in Figure 5b,d. The main color of allanite is yellowish brown, with an obvious band texture observed in the BSE image. The main paragenetic minerals of allanite include zircon ± garnet ± titanite ± pyrochlore.

5. Discussion

At present, the previous studies have shown that magmatism can enrich Nb in some ore deposits to the available grade [22,23]. On the other hand, there is sufficient evidence that the hydrothermal process may play a more important role in Nb enrichment and mineralization in many rare metal deposits [9,24–26]. Likewise, hydrothermal alteration also occurs widely in Shuangshan alkaline rocks, such as albitization, calcification, and silicification [15]. The extensive occurrence of hydrothermal alteration has changed the structures of the primary minerals and mineral assemblage. For example, type-2 pyrochlore and type-2 zircon have obvious metasomatic structures and dissolution holes. The dissolution-reprecipitation structure proves the existence of mineral replacement actions [27]. At the same time, the difference in chemical compositions between the altered minerals (pyrochlore and zircon) and magmatic (precursor) minerals also proves the transformation of minerals by hydrothermal fluid. Based on the textural features and chemical compositions of pyrochlores and zircons, we call these type-1 pyrochlore, type-1 zircon magmatic pyrochlore, and magmatic zircon, respectively, and these altered minerals (type-2 pyrochlore and type-2 zircon) are hydrothermal pyrochlore and hydrothermal zircon, respectively.

5.1. Magma Evolution and Pyrochlore Crystallization

Pyrochlore is an important ore mineral found in alkaline Nb deposits, and it is the main Nb-bearing mineral found in the Strange Lake deposit in Canada, Khaldzan-Buregtey complex in Mongolia, and Baerzhe rare metal deposit of Inner Mongolia in China [11,28,29]. In these deposits, the primary pyrochlore is generally found to be subhedral-euhedral or acicular, distributed among the grains of the rock-forming minerals or as mineral inclusions, and a few of them have been associated with Zr-bearing accessory minerals. In the nepheline syenite of the Shuangshan complex, we also observed the primary pyrochlore, which should be the product of magmatic crystallization. In fact, due to the high concentrations of volatiles, such as F in alkaline magma, and the geochemical properties of HFSE, certain HFSE, such as Nb and Zr, tend to be enriched in the residual melt in the late stage [30]. The concentration of Nb in the magma reached saturation in the late stage of evolution, resulting in the crystallization of a small amount of the primary pyrochlore in many alkaline complexes [23,31].

The primary pyrochlore in the Shuangshan nepheline syenite has late overgrown pyrochlore on its surface (Figure 3b). Similarly, in the Strange Lake deposit, Siegel et al. (2018) found the phenomenon of overgrown pyrochlore on the primary pyrochlore. The overgrown and early crystallized pyrochlores were similar in composition, such as light Rare Earth Element (LREE) enrichment. However, the concentrations of Ba, Pb, Si, and other elements of the overgrown pyrochlore changed. They believed that these two types of pyrochlores were the result of magma differentiation and evolution [23]. With the crystallization differentiation of magma, its composition changed, thus changing in the composition of the overgrown pyrochlore. The change in the composition of pyrochlore in the Shuangshan syenite may also indicate the direction of evolution of Shuangshan alkaline magma. As shown in Figure 4, there was an obvious negative correlation between SiO_2 and Nb_2O_5. This phenomenon may indicate that Si was incorporated in the structure of the pyrochlore during crystallization of the magma, and Si occupied the octahedral sites of the pyrochlore structure and replaced position B in the normal pyrochlore AB_2X_6Y [32,33]. When magma crystallized continuously, the alkalinity of the residual melt continuously increased, and the volatiles also accumulated in the residual melt. The decrease in the Si concentration in the pyrochlore may have been due to the formation of the Shuangshan

nepheline syenite itself in a silicon-unsaturated system. With the crystallization of alkaline amphibole, alkaline feldspar, and other rock-forming minerals, the concentration of silicon in the melt also decreased, resulting in a low Si concentration in the overgrown pyrochlore.

5.2. Hydrothermal Alteration

It has been generally believed that Nb, Zr, and other HFSE cannot easily migrate via hydrothermal fluids, and thus they have often been used for geochemical tracing. However, an increasing number of studies have shown that HFSE can migrate via some specific hydrothermal fluids, those containing anions such as F and Cl, and especially those containing F. Zr can form a stable complex with F to aid in migration [11]. Similarly, Nb can also combine with F in hydrothermal fluids to form stable complexes, such as $Nb(OH)_2F_3$, with the solubility of Nb in hydrothermal fluids containing F reaching 10 ppm or even higher [34,35]. After hydrothermal alteration, the primary HFSE minerals transform or form new mineral types, such as primary Nb-rich zircon and eudialyte and elpidite transformed into fergusonite-(Y), fergusonite, and armstrongite or gittinsite, respectively [14,36]. In this process, the newly formed minerals and mineral assemblages were controlled by the primary mineral composition and hydrothermal composition.

As mentioned above, in addition to magmatic pyrochlore, we also found hydrothermal pyrochlore closely associated with zircon in the Shuangshan nepheline syenite. A comparison between the main compositions of magmatic and hydrothermal pyrochlores in Shuangshan nepheline syenite revealed that the latter contained higher F, Ca, and Na contents and a lower Si content, indicating that the formation of this pyrochlore was probably affected by the late F-, Na-, and Ca-bearing hydrothermal fluid. On the other hand, we also found fluorite veins filling the rock-forming minerals in thin sections. Combined with the close spatial relationship between this hydrothermal pyrochlore and zircon (Figures 3d and 4d), we speculated that this type of pyrochlore was formed by hydrothermal alteration, and Nb in the aggregate pyrochlore migrated from Nb-rich primary zircon. The entry of Ca- and Na-containing hydrothermal fluid led to the dissolution of zircon, and the released Nb formed $Nb(OH)_2F_3$. Then, the Ca and Na in the hydrothermal fluid reacted with $Nb(OH)_2F_3$ to finally form the hydrothermal pyrochlore. The following reactions took place:

$$ZrSiO_4 \bullet NbSiO_4{}^+ \text{ (Nb-bearing zircon)} + 3F^- + H_2O = ZrSiO_4 \text{ (zircon)} + Nb(OH)_2F_3 + SiO_3{}^{2-} \quad (1)$$

$$4Nb(OH)_2F_3 + 7Ca^{2+} + 2Na^+ + 16OH^- = 2CaNaNb_2O_6F \text{ (pyrochlore)} + 5CaF_2 + 12H_2O \quad (2)$$

Simultaneously, other minerals were also altered by this Na- and Ca-bearing hydrothermal fluid. For example, nepheline was observed to be altered into cancrinite, especially nepheline adjacent to the aggregate pyrochlore, and this type of cancrinite often contained a higher amount of water (~10 wt.%):

$$3KNa_3[AlSiO_4]_4 \text{ (nepheline)} + 2CaCO_3 + 2Ca^{2+} + 4OH^- + 3Na^+ = 2Na_6Ca_2[AlSiO_4]_6[CO_3](OH)_2 \text{ (cancrinite)} + 3K \quad (3)$$

A small amount of zircon was altered into gittinsite as follows:

$$ZrSiO_4 \text{ (zircon)} + Ca^{2+} + SiO_3{}^{2-} = CaZrSi_2O_7 \text{ (gittinsite)} \quad (4)$$

This widespread calcification alteration proved that the Shuangshan nepheline syenite was affected by the late Na- and Ca-bearing hydrothermal fluid, and its presence evidently impacted the mobilization, migration, and re-enrichment of Nb as a pyrochlore. In the Shuangshan nepheline syenite, the hydrothermal pyrochlore was only found in the interior of the altered zircon or close to zircon, which was because of the difficultly of HFSE, such as Nb, to be transported long distances via hydrothermal fluid. Nb-bearing minerals, such as columbite and fergusonite, which formed after the hydrothermal alteration were usually formed in situ or only migrated at the micron scale [7].

The primary zircon was dissolved via a hydrothermal process where fluorine likely migrated Nb as a complex. However, a comparison between the compositions of the mag-

matic and hydrothermal zircons revealed no significant difference in the Nb concentrations. It can be seen from Figure 6 that the lowest Nb concentration in the hydrothermal zircon remained higher than that in the magmatic zircon after the migration of some Nb due to the dissolution of hydrothermal fluid. This may be because the migration of Nb via hydrothermal fluid was limited, and the latter could not completely remove the Nb in the zircon.

5.3. Quantitative Evaluation of the Migration of Niobium from Hydrothermal Zircon and Titanite

In the previous discussion, we provided the evidence that the hydrothermal pyrochlore in the Shuangshan nepheline syenite was formed by Nb recrystallization that migrated from Nb-rich zircon under the action of late Na- and Ca-bearing hydrothermal fluid. To determine the amount of Nb that could be reserved by zircon on its crystallization, we carried out a simple quantitative calculation.

In addition to pyrochlore and zircon, titanite also contains a high amount of Nb (Table 3), which is also the main niobium-bearing mineral. According to our whole rock chemistry data (Appendix A, Table A2), the mass fractions of zircon and titanite were calculated. Based on the distribution coefficient of niobium in various minerals [37] and the solubility of pyrochlore [38], the mass fractions of niobium in rock-forming minerals, pyrochlore, zircon, and titanite were estimated. As shown in Table 4, when nepheline syenite crystallized at 600 °C [38], titanite and zircon accounted for 20.05 wt.% and 2.81 wt.% of the total Nb_2O_5 content, respectively. Pyrochlore accounted for 67.56 wt.% of the total Nb_2O_5 content, and the remainder was in rock-forming minerals, such as alkali feldspar, feldspathoid, biotite, amphibole, and magnetite. In addition, the lowest crystallization temperature of the Shuangshan nepheline syenite calculated by Zhu et al. (2020) was 500 °C. Therefore, we also estimated the mass fraction of niobium in each mineral phase at 500 °C (Table 4). The Nb contents of titanite and zircon were 30.07 wt.% and 0.42 wt.%, respectively, while the Nb crystallized in the form of a pyrochlore accounted for 95.13 wt.%, and only a little niobium entered the rock-forming minerals. In other words, as the host minerals of Nb in the magmatic stage, the capacities of zircon and titanite for Nb in the Shuangshan nepheline syenite were significantly limited.

Table 4. The concentration of Nb in minerals of the Shuangshan nepheline syenite.

Temperature	**600 °C**	**500 °C**	
Total Content of Nb_2O_5 in Nepheline Syenite (ppm)			
Initially in melt	1000	1000	
At pyrochlore saturation	1000	150	
Nb_2O_5 Content of Minerals (ppm)			D_{Nb} *
K-feldspar (60%)	18.00	2.70	0.03
Albite (10%)	3.00	0.45	0.03
Nepheline (20%)	6.00	0.90	0.03
Amphibole (4%)	3.76	0.56	0.094
Biotite (2%)	64.00	9.60	3.2
Titanite (1.23%)	200.49	30.07	16.3
Magnetite (1%)	1.10	0.17	0.11
Zircon (0.72%)	28.08	4.21	3.9
Pyrochlore	675.57	951.34	
Nb_2O_5 in other minerals (ppm)	324.43	48.66	
Nb as pyrochlore (% of total)	67.56	95.13	

Note: * D_{Nb} of orthoclase, albite, nepheline, amphibole, biotite, and magnetite from Ballouard et al. (2020) or calculated based on their experiment data. D_{Nb} of zircon and titanite is obtained by calculation of the analysis data of our sample.

It is evident that the concentration of zirconium (ZrO_2 0.1–0.4 wt.%, Appendix A (Table A2)) in the Shuangshan nepheline syenite was significantly lower than that in the same type of rare metal deposit, such as the Nechalacho rare metal deposit (ZrO_2 2.1–2.99 wt.%) [7]. Therefore,

the evidence showed that Nb in the Shuangshan alkaline complex was mainly preserved in the magmatic pyrochlore. Although a small amount of Nb can be removed from zircon (or titanite) by a later hydrothermal process, this effect was very limited for the re-enrichment of Nb.

6. Conclusions

In the Shuangshan deposit, the magmatic and deuteric pyrochlore have different textural and chemical characteristics. Magmatic pyrochlores are euhedral crystals with small sizes which are generally found in orthoclase and albite mineral grains. Contrarily, hydrothermal pyrochlores are almost associated with aggregate zircon ± allanite ± magnetite, and the diameters of the large mineral aggregates can reach the millimeter level. Nearly all aggregate mineral assemblages are found in the mineral grains of cancrinite or adjacent to cancrinite. In terms of compositions, the Na, Ca, and F concentrations in the hydrothermal pyrochlore were higher than those of the magmatic pyrochlore.

The hydrothermal pyrochlore origin is related to the alteration of late Na and Ca-rich fluid. In the process of alteration, the addition of Na- and Ca-bearing hydrothermal fluid alters both the F-rich minerals and the adjacent Nb-bearing zircon. Nb is released from zircon by hydrothermal fluid, and it finally forms an aggregate pyrochlore with aggregate zircon. However, the quantitative calculation shows that the amount of Nb reserved by zircon is very small. Therefore, this study suggests that hydrothermal alteration plays a certain role in the redistribution of Nb, but the enrichment of Nb is limited. The Shuangshan deposit is a significant Nb resource as a result of the concentration of this metal by magmatic processes.

Author Contributions: Conceptualization, H.W. and Y.T.; methodology, H.W. and Y.T.; validation, H.Z. and Y.T.; investigation, H.W., Y.-S.X., and S.-X.Q.; resources, Y.-W.S.; data curation, Z.-H.L.; writing—original draft preparation, H.W.; writing—review and editing, Y.T. and Z.-H.L. All authors have read and agreed to the published version of the manuscript.

Funding: This research was funded by the Natural Science Foundation of China, grant numbers 41773053 and 91962222.

Acknowledgments: We gratefully thank the Henan Institute of Geological Survey for support in the fieldwork. We would like to thank the State Key Laboratory of Ore Deposit Geochemistry of the Chinese Academy of Sciences for their help in the EPMA and BSE analyses.

Conflicts of Interest: The authors declare no conflict of interest.

Appendix A

Table A1. Standards used for electron microprobe analyses (the standard used for a given element was employed for all minerals analyzed unless otherwise noted).

Standard	Element	Counting Time (s)
Pyrope	Fe, Mn, Ti, Al, Si, Ca	15
Benitoite	Ba	15
Orthoclase	Na, K	15
Monazite	Y, La, Ce	45
Apatite	F	15
Anhydride	Sr	45
PbS	Pb	15
Cubic Zirconia [1]	Zr, Hf, Y	15,45
Rutile [2]	Ti	15
Diopside [2]	Ca	15
Albite [3]	Na, Al, Si	15
Almandine [4]	Fe	15
Kaersutite [4]	Na, Ca, Ti, Al, Si, Mg, K	15
MAC-Nb	Nb	15
MAC-Ta	Ta	15
MAC-U	U	45

[1] Zircon. [2] Titanite. [3] Nepheline. [4] Taramite.

Table A2. Major element composition and Rare Earth Elements (REEs) + Zr and Nb composition of Shuangshan nepheline syenite. The major element and trace element were obtained by X-ray fluorescence (XRF) and ICP-MS, respectively, at the State Key Laboratory of Ore Deposit Geochemistry of the Chinese Academy of Sciences.

Sample	DZ18-02	DZ18-06	DZ18-08	DZ18-09	DZ18-18	DZ18-21	DZ18-28	DZ18-30	ZK503-6
					Oxide (wt%)				
SiO_2	57.26	56.70	60.38	57.53	56.99	52.66	56.76	56.81	56.11
Al_2O_3	19.17	21.23	21.37	17.73	20.10	16.55	19.75	19.30	19.82
TFe_2O_3	4.61	4.29	3.62	5.44	3.96	6.56	5.48	5.20	5.04
MgO	0.75	0.72	0.32	0.55	0.46	0.85	0.69	0.71	0.37
CaO	2.72	1.49	0.25	3.13	1.30	7.20	1.82	2.39	1.94
Na_2O	6.80	5.57	7.44	5.87	3.72	4.43	6.21	7.54	7.88
K_2O	6.00	6.68	4.12	7.05	8.87	6.00	6.70	5.97	5.27
MnO	0.33	0.41	0.37	0.52	0.34	0.49	0.40	0.35	0.25
P_2O_5	0.05	0.05	0.05	0.05	0.09	0.20	0.04	0.05	0.05
TiO_2	0.47	0.26	0.30	0.43	0.64	0.38	0.58	0.52	0.50
LOI	1.51	1.66	0.99	1.21	2.62	3.83	0.68	0.98	1.67
Total	99.67	99.07	99.21	99.51	99.09	99.15	99.11	99.83	98.90
					Trace element (μg/g)				
La	140	257	279	261	318	684	248	398	531
Ce	254	458	458	435	603	1431	358	627	791
Pr	23	36	42	41	62	160	30	53	68
Nd	72	105	123	123	206	553	82	154	190
Sm	10	15	17	17	29	80	11	20	25
Eu	1	1	2	2	3	9	1	2	3
Gd	9	13	15	15	24	63	11	18	23
Tb	2	2	2	2	3	9	2	3	3
Dy	12	11	16	15	19	51	11	17	20
Ho	3	3	4	3	4	10	2	4	4
Y	84	69	120	108	120	285	79	118	137
Er	8	8	12	11	12	29	8	12	14
Tm	1	1	2	2	2	4	1	2	2
Yb	8	12	15	14	13	24	8	14	15
Lu	1	2	2	2	2	3	1	2	2
Zr	1143	3447	2529	2305	1748	1230	2109	2568	3642
Nb	232	531	787	546	511	729	451	582	703

References

1. Salvi, S.; Williams-Jones, A.E. Alkaline granite-syenite deposits. In *Rare-Element Geochemistry and Mineral Deposits*; Linnen, L., Samson, I.M., Eds.; Geological Association of Canada: St. John's, NL, Canada, 2005; pp. 315–341.
2. Linnen, R.L.; Samson, I.M.; Williams-Jones, A.E.; Chakhmouradian, A.R. Geochemistry of the Rare-Earth Element, Nb, Ta, Hf, and Zr Deposits. In *Treatise on Geochemistry*, 2nd ed.; Elsevier: Amsterdam, The Netherlands, 2014; pp. 543–568. [CrossRef]
3. Huang, H.; Wang, T.; Zhang, Z.; Li, C.; Qin, Q. Highly differentiated fluorine-rich, alkaline granitic magma linked to rare metal mineralization: A case study from the Boziguo'er rare metal granitic pluton in South Tianshan Terrane, Xinjiang, NW China. *Ore Geol. Rev.* **2018**, *96*, 146–163. [CrossRef]
4. Vasyukova, O.; Williams-Jones, A.E. Fluoride–silicate melt immiscibility and its role in REE ore formation: Evidence from the Strange Lake rare metal deposit, Québec-Labrador, Canada. *Geochim. Cosmochim. Acta* **2014**, *139*, 110–130. [CrossRef]
5. Vasyukova, O.; Williams-Jones, A.E. The evolution of immiscible silicate and fluoride melts: Implications for REE ore-genesis. *Geochim. Cosmochim. Acta* **2016**, *172*, 205–224. [CrossRef]
6. Bailey, J.; Sorensen, H.; Andersen, T.; Kogarko, L.; Rosehansen, J. On the origin of microrhythmic layering in arfvedsonite lujavrite from the Ilímaussaq alkaline complex, South Greenland. *Lithos* **2006**, *91*, 301–318. [CrossRef]
7. Sheard, E.R.; Williams-Jones, A.E.; Heiligmann, M.; Pederson, C.; Trueman, D.L. Controls on the Concentration of Zirconium, Niobium, and the Rare Earth Elements in the Thor Lake Rare Metal Deposit, Northwest Territories, Canada. *Econ. Geol.* **2012**, *107*, 81–104. [CrossRef]
8. Gysi, A.P.; Williams-Jones, A.E. Hydrothermal mobilization of pegmatite-hosted REE and Zr at Strange Lake, Canada: A reaction path model. *Geochim. Cosmochim. Acta* **2013**, *122*, 324–352. [CrossRef]
9. Salvi, S.; Fontan, F.; Monchoux, P.; Williams-Jones, A.E.; Moine, B. Hydrothermal mobilization of high field strength elements in alkaline igneous systems: Evidence from the Tamazeght complex (Morocco). *Econ. Geol. Bull. Soc.* **2000**, *95*, 559–575. [CrossRef]

10. Salvi, S.; Williams-jones, A.E. The Role of Hydrothermal Processes in the Granite-Hosted Zr, Y, Ree Deposit at Strange Lake, Quebec Labrador—Evidence from Fluid Inclusions. *Geochim. Cosmochim. Acta* **1990**, *54*, 2403–2418. [CrossRef]
11. Salvi, S.; Williams-Jones, A.E. The role of hydrothermal processes in concentrating high-field strength elements in the Strange Lake peralkaline complex, northeastern Canada. *Geochim. Cosmochim. Acta* **1996**, *60*, 1917–1932. [CrossRef]
12. Salvi, S.; Williams-Jones, A.E. Alteration, HFSE mineralisation and hydrocarbon formation in peralkaline igneous systems: Insights from the Strange Lake Pluton, Canada. *Lithos* **2006**, *91*, 19–34. [CrossRef]
13. Adam, J.; Green, T. The influence of pressure, mineral composition and water on trace element partitioning between clinopyroxene, amphibole and basanitic melts. *Eur. J. Mineral.* **2003**, *15*, 831–841. [CrossRef]
14. Timofeev, A.; Williams-Jones, A.E. The Origin of Niobium and Tantalum Mineralization in the Nechalacho REE Deposit, NWT, Canada. *Econ. Geol.* **2015**, *110*, 1719–1735. [CrossRef]
15. Zhang, S.; Zhang, B.; Yuming, Z.; Junkui, C.; Danfeng, H.; Shanpo, L. Discovery of fergusonite from Dazhuang niobium rare earth deposit in Henan Province and its geological significance. *Glob. Geol.* **2020**, *39*, 282–293.
16. Zhu, Y.-X.; Wang, L.-X.; Ma, C.-Q.; Wiedenbeck, M.; Wang, W. The Neoproterozoic alkaline rocks from Fangcheng area, East Qinling (China) and their implications for regional Nb mineralization and tectonic evolution. *Precambrian Res.* **2020**, *350*, 105852. [CrossRef]
17. Bao, Z.; Wang, Q.; Bai, G.; Zhao, Z.; Song, Y.; Liu, X. Geochronology and geochemistry of the Fangcheng Neoproterozoic alkali-syenites in East Qinling orogen and its geodynamic implications. *Sci. Bull.* **2008**, *53*, 2050–2061. [CrossRef]
18. Dong, Y.; Santosh, M. Tectonic architecture and multiple orogeny of the Qinling Orogenic Belt, Central China. *Gondwana Res.* **2016**, *29*, 1–40. [CrossRef]
19. Wang, X.; Wang, T.; Zhang, C. Neoproterozoic, Paleozoic, and Mesozoic granitoid magmatism in the Qinling Orogen, China: Constraints on orogenic process. *J. Asian Earth Sci.* **2013**, *72*, 129–151. [CrossRef]
20. Zhang, Z.; Zhu, B.; Chang, X.; Xie, J. Major element characteristics of the alkali-rich intrusive rocks zone and distribution of the subzones in the northern part of east Qinling, China. *Acta Petrol. Sin.* **2002**, *18*, 468–474.
21. Zhang, Z.; Zhu, B.; Chang, X. Nd, Sr, Pb isotopic geochemistry of the alkali-rich intrusive rocks in East Qinling, central China and its tectonic significance. *Geochimica* **2000**, *029*, 455–461.
22. Moller, V.; Williams-Jones, A.E. Petrogenesis of the Nechalacho Layered Suite, Canada: Magmatic Evolution of a REE–Nb-rich Nepheline Syenite Intrusion. *J. Petrol.* **2016**, *57*, 229–276. [CrossRef]
23. Siegel, K.; Vasyukova, O.V.; Williams-Jones, A.E. Magmatic evolution and controls on rare metal-enrichment of the Strange Lake A-type peralkaline granitic pluton, Québec-Labrador. *Lithos* **2018**, *308–309*, 34–52. [CrossRef]
24. Kim, E.J.; Yang, S.J.; No, S.G.; Park, S.W.; Lee, S.R.; Kim, Y.D.; Jo, J. The characteristics of zircon as the evidence for post-magmatic remobilization of REE and HFSE in the northern Motzfeldt alkaline igneous complex, southern Greenland. *Geosci. J.* **2018**, *22*, 921–938. [CrossRef]
25. Schmitt, A.K.; Trumbull, R.B.; Dulski, P.; Emmermann, R. Zr-Nb-REE mineralization in peralkaline granites from the Amis Complex, Brandberg (Namibia): Evidence for magmatic pre-enrichment from melt inclusions. *Econ. Geol. Bull. Soc.* **2002**, *97*, 399–413. [CrossRef]
26. Vasyukova, O.V.; Williams-Jones, A.E.; Blamey, N.J.F. Fluid evolution in the Strange Lake granitic pluton, Canada: Implications for HFSE mobilisation. *Chem. Geol.* **2016**, *444*, 83–100. [CrossRef]
27. Putnis, A. Mineral replacement reactions: From macroscopic observations to microscopic mechanisms. *Mineral. Mag.* **2018**, *66*, 689–708. [CrossRef]
28. Kempe, U.; Möckel, R.; Graupner, T.; Kynicky, J.; Dombon, E. The genesis of Zr–Nb–REE mineralisation at Khalzan Buregte (Western Mongolia) reconsidered. *Ore Geol. Rev.* **2015**, *64*, 602–625. [CrossRef]
29. Yang, W.B.; Niu, H.C.; Shan, Q.; Luo, Y.; Qiu, Y.Z. Ore-forming mechanism of the Baerzhe super-large rare and rare earth elements deposit. *Acta Petrol. Sin.* **2009**, *25*, 2924–2932.
30. Keppler, H. Influence of Fluorine on the Enrichment of High-Field Strength Trace-Elements in Granitic-Rocks. *Contrib. Mineral. Petrol.* **1993**, *114*, 479–488. [CrossRef]
31. Moller, V.; Williams-Jones, A.E. Magmatic and Hydrothermal Controls on the Mineralogy of the Basal Zone, Nechalacho REE-Nb-Zr Deposit, Canada. *Econ. Geol.* **2017**, *112*, 1823–1856. [CrossRef]
32. Bonazzi, P. Single-crystal diffraction and transmission electron microscopy studies of "silicified" pyrochlore from Narssarssuk, Julianehaab district, Greenland. *Am. Mineral.* **2006**, *91*, 794–801. [CrossRef]
33. Atencio, D.; Andrade, M.B.; Christy, A.G.; Giere, R.; Kartashov, P.M. The Pyrochlore Supergroup of Minerals: Nomenclature. *Can. Mineral.* **2010**, *48*, 673–698. [CrossRef]
34. Timofeev, A.; Migdisov, A.A.; Williams-Jones, A.E. An experimental study of the solubility and speciation of niobium in fluoride-bearing aqueous solutions at elevated temperature. *Geochim. Cosmochim. Acta* **2015**, *158*, 103–111. [CrossRef]
35. Akinfiev, N.N.; Korzhinskaya, V.S.; Kotova, N.P.; Redkin, A.F.; Zotov, A.V. Niobium and tantalum in hydrothermal fluids: Thermodynamic description of hydroxide and hydroxofluoride complexes. *Geochim. Cosmochim. Acta* **2020**, *280*, 102–115. [CrossRef]
36. Salvi, S.; Williamsjones, A.E. Zirconosilicate Phase-Relations in the Strange Lake (Lac-Brisson) Pluton, Quebec-Labrador, Canada. *Am. Mineral.* **1995**, *80*, 1031–1040. [CrossRef]

37. Ballouard, C.; Massuyeau, M.; Elburg, M.A.; Tappe, S.; Viljoen, F.; Brandenburg, J.-T. The magmatic and magmatic-hydrothermal evolution of felsic igneous rocks as seen through Nb-Ta geochemical fractionation, with implications for the origins of rare-metal mineralizations. *Earth-Sci. Rev.* **2020**, *203*, 103115. [CrossRef]
38. McNeil, A.G.; Linnen, R.L.; Flemming, R.L. Solubility of wodginite, titanowodginite, microlite, pyrochlore, columbite-(Mn) and tantalite-(Mn) in flux-rich haplogranitic melts between 700 °C and 850 °C and 200 MPa. *Lithos* **2020**, *352–353*, 105239. [CrossRef]